Distribution Agreement

In presenting this thesis as a partial fulfillment of the requirements for a degree from Emory University, I hereby grant to Emory University and its agents the non-exclusive license to archive, make accessible, and display my thesis in whole or in part in all forms of media, now or hereafter now, including display on the World Wide Web. I understand that I may select some access restrictions as part of the online submission of this thesis. I retain all ownership rights to the copyright of the thesis. I also retain the right to use in future works (such as articles or books) all or part of this thesis.

Lilian Daniela Galarza Paez March 23, 2022

Nonselective Cation Channels Maintain Alveolar Fluid Clearance After Exposure to Toxins from Respiratory Pathogens

by

Lilian Daniela Galarza Paez

Douglas C. Eaton
Adviser

Department of Biology

Douglas C. Eaton

Adviser

Michael Koval

Committee Member

Nicole Gerardo

Committee Member

2022

Nonselective Cation Channels Maintain Alveolar Fluid Clearance After Exposure to Toxins from Respiratory Pathogens

By

Lilian Daniela Galarza Paez

Douglas C. Eaton

Adviser

An abstract of
a thesis submitted to the Faculty of Emory College of Arts and Sciences
of Emory University in partial fulfillment
of the requirements of the degree of
Bachelor of Science with Honors

Department of Biology

2022

Abstract

Nonselective Cation Channels Maintain Alveolar Fluid Clearance After Exposure to Toxins from Respiratory Pathogens
By Lilian D. Galarza Paez

Normal gas exchange in the alveoli is facilitated by a thin fluid layer. This layer is carefully regulated by two ion channels: highly selective cation channels (HSC/ENaC) and nonselective cation channels (NSC). Previous research found that both channels contribute about equally to alveolar fluid clearance (AFC). Since the molecular composition of NSC is a recent discovery, not much is known about NSC's response to various respiratory pathogens. NSC are composed of an alpha-ENaC subunit and at least one acid-sensing ion channel 1a (ASIC1a) subunit. Our study aims are to understand how NSC contribute to alveolar epithelial permeability and how the lungs respond to toxins from respiratory pathogens. We hypothesize that AFC will be lower in the absence of ASIC1a (ASIC1 KO) when exposed to toxins from respiratory pathogens: Lipopolysaccharide (LPS) from E. coli and Pneumolysin (PLY) from P. pneumoniae. Additionally, we hypothesize that ASIC1 KO animals will have increased baseline alveolar epithelial permeability. All animal protocols were approved by Emory's IACUC.

We introduced pathogen toxins via intratracheal instillation or intraperitoneal injections to ASIC1 KO (KO) and wildtype (WT) mouse models. We determined AFC through changes in the concentrations of Evans Blue (EB) or Fluorescein isothiocyanate–dextran (FITC-dextran) in instillates. Permeability of capillaries and alveolar epithelium were investigated by looking at dye accumulation in pulmonary tissue. Concentrations were determined using spectrophotometry. Our findings suggest that LPS and PLY inhibit all HSC-related AFC leaving only NSC-associated AFC. The AFC of LPS and PLY treated KO animals is lower than AFC for

LPS treated WT animals. Neither HSC nor NSC are fully functioning or contributing to AFC in toxin treated groups. Observations on permeability are preliminary but suggest fluid accumulation in the interstitium for the ASIC1 KO group.

Collectively, these results suggest that the regulation of the alveolar fluid layer is dependent on the function of NSC especially after exposure to toxins. HSC and NSC appear to contribute to alveolar permeability and pulmonary capillary integrity but more research is needed. Our findings can help guide treatment for alveolar flooding caused by toxins from different respiratory pathogens by elucidating their mechanism of action.

Nonselective Cation Channels Maintain Alveolar Fluid Clearance After Exposure to Toxins from Respiratory Pathogens

By

Lilian Daniela Galarza Paez

Douglas C. Eaton

Adviser

A thesis submitted to the Faculty of Emory College of Arts and Sciences
of Emory University in partial fulfillment
of the requirements of the degree of
Bachelor of Science with Honors

Department of Biology

2022

Acknowledgements

First and foremost, I would like to thank my advisor and mentor, Dr. Douglas C. Eaton for his help, guidance, and support throughout my undergraduate career. I would also like to thank all of the Eaton Lab members particularly, Dr. Chang Song and Auriel Moseley, whose technical and ethical guidance was essential for this project and my growth as a scientist. I would like to thank Qiang Yue for helping me understand single-channel measurements and contributing to my work. I would also like to thank the members of my committee Dr. Michael Koval and Dr. Nicole Gerardo for their time and invaluable feedback. Finally, I would never have made it through this process without the constant support and encouragement of Jonah, my parents, Celia and Luis, my sisters, Liz and Laura, and my grandfather, Carlos—thank you.

Table of Contents

Introduction 1

The alveolar fluid layer is critical for respiration. 1

Fluid must be in a steady state across alveolar compartments 1

HSC and NSC maintain AFC. 2

High wet weight-to-dry weight lung ratios suggest fluid accumulation in the interstitium. 3

HSC and NSC show differing responses to stimuli. 3

LPS and PLY have an impact on ENaC/HSC. 4

PLY impairs epithelial and endothelial function. 5

Study aims. 6

Materials and Methods 7

Animals. 7

Chemicals and reagents 7

Intratracheal Instillations. 7

Intraperitoneal Injections. 8

Alveolar fluid clearance. 8

Evans blue capillary permeability assay. 9

Wet weight-to-dry weight ratios. 11

Alveolar epithelial permeability. 11

Single-channel, patch-clamp analysis. 12

Statistical analysis. 13

NSC contribute about equally to AFC. 14

LPS and PLY block HSC-associated AFC. 15
Acute PLY in alveolar type II cells suppresses HSC activity. 15
ASIC1 KO mice have more fluid in their lungs. 16
Capillary permeability may be impacted by LPS. 16
Forty KDa FITC-dextran is a measure of AFC. 17
FITC-dextran is a measure of epithelial permeability. 17
Discussion 19
NSC are significant contributors to lung fluid balance. 19
LPS and PLY act on ENaC/HSC to inhibit fluid clearance. 20
NSC and HSC have contrasting responses to acute PLY. 21
Endotoxins may compromise the integrity of epithelial barriers. 22
Summary: NSC are important for proper lung function, especially after endotoxin exposure. 25
Figures 26
Figure 1. A schematic diagram of an alveolus. 26
Figure 2. Genetic knockout of nonselective cation channels (NSC) and pharmacological blockage of highly-selective cation channels (HSC) decreases alveolar fluid clearance (AFC). 28
Figure 3. Highly-selective cation channel (HSC)-related fluid clearance is different in male and female wild type mice. 30
Figure 4. Lipopolysaccharide (LPS) inhibits highly-selective cation channel (HSC)-related alveolar fluid clearance (AFC) 31
Figure 5. Pneumolysin (PLY) inhibits highly-selective cation channel (HSC)-related alveolar fluid clearance (AFC). AFC of wild type and PLY treated wild type are 32

Figure 6. Pneumolysin (PLY) causes a significant increase in the open probability of nonselective cation channels (NSC) on alveolar type 2 cells as assessed by single-patch clamp analysis..... 33
Figure 8. ASIC1 KO have fluid accumulation in their interstitium..... 35
Figure 9. Forty KDa FITC-dextran detects decreases in fluid clearance caused by endotoxins alveolar fluid clearance (AFC) in wild type mice..... 37
Figure 10. Different molecular weight FITC-dextran cross the alveolar epithelial to different degrees 38
Figure 11. FITC-dextran is a measure of epithelial permeability. 39
References..... 40

Introduction

The alveolar fluid layer is critical for respiration.

The human lungs have approximately 500 million alveoli which are the site of gas exchange with the blood. The alveolar epithelium is lined by a thin fluid layer that is necessary for normal gas exchange; thus, the thickness and composition of this layer must be carefully maintained. Disruption of the alveoli's fluid layer can result in lung edema and alveolar flooding [1]. These potentially lethal symptoms are characteristic of pathologies such as influenza, COVID-19, pneumonia, acute lung injury, and cystic fibrosis. Due to its critical role in the respiratory system, the human alveolar epithelium is an increasingly important area of interest.

Fluid must be in a steady state across alveolar compartments.

The alveoli system has five distinct components: the alveolar lumen, the intercellular compartments of the polarized alveolar epithelial cells, tight junctions and the paracellular pathway, the basolateral interstitium, and the pulmonary capillaries (Figure 1) [2]. Regulation of the alveolar epithelium is aided by tight junctions, or zonulae occludentes, whose function is to limit paracellular pathways. The combination of the tight junctions and the high resistance of the luminal membranes of the epithelial cells causes the alveolar epithelium to be the main barrier to salt and water movement in the alveolar system. In contrast, the pulmonary capillary endothelium is relatively permeable to the movement of salt, water, and serum proteins.

Consequently, osmotic and hydrostatic pressures of the pulmonary capillary drive fluid through the interstitium into the alveolar lumen. Simultaneously, sodium (Na^+) and chloride (Cl^-) ions flow from high concentrations in the capillary into the alveolar lumen through the channels in tight junctions [3]. To regulate the entry of this large fluid volume, Na^+ and Cl^- move down

their electrical and concentration gradients into the intercellular compartment of alveolar epithelial cells through cation and anion channels embedded in the lumenal membrane of these cells. On the basolateral membrane of epithelial cells, sodium/potassium pumps facilitate the active movement of Na^+ back into the interstitium [4]. The movement of cationic Na^+ drives the movement of anionic Cl^-. The osmotic gradient produced by the Na^+ and Cl^- drives the movement of water through the epithelial cells and enough flows into the capillaries to prevent flooding in the alveoli. The ideal thickness of the fluid layer is maintained as Na^+ and Cl^- move back into the alveolar lumen through tight junction channels, whose permeability changes based on environmental and pathological stressors [5]. During normal movement of fluid out of the alveolar lumen, known as alveolar fluid clearance (AFC), the concentration of these ions and water volume is in a steady state in all four compartments. However, pulmonary edema caused by respiratory pathogens results in insufficient transport of fluid out of the alveolar lumen [6]. The pathway through which these pathologies result in edema is not yet completely clear.

HSC and NSC maintain AFC.

Cation channels are critical to the process described above, and two have been identified in the lung: Highly Selective Cation Channels (HSC) and Nonselective Cation Channels (NSC). Both of these channels are expressed in both Alveolar Type I (AT1) and Alveolar Type II (AT2) cells of the alveolar epithelium [7]. Epithelial Sodium Channels (ENaC) are responsible for all Na^+ transport in other Na^+-transporting epithelia such as the kidneys. Not surprisingly, HSC have been identified as ENaC which are composed of three homologous subunits, $\alpha, \beta,$ and γ [8]. The composition of NSC has only recently been elucidated and is thought to include the α-ENaC subunit and one or more Acid Sensing Ion Channel (ASIC) 1a subunits [9]. A previous study

used a genetically modified mouse model lacking expression of ASIC1 to show that both channels contribute about equally to AFC [10]. Additionally, amiloride, known to block HSC, results in an AFC decrease of about half suggesting that NSC are also aiding in returning fluid from the alveolar lumen [11].

High wet weight-to-dry weight lung ratios suggest fluid accumulation in the interstitium.

ASIC1 knockout mice have decreased alveolar fluid clearance but present as seemingly healthy without any noticeable respiratory discomfort. However, analysis of their wet lung weight-to-dry lung weight ratios revealed more fluid than could be accounted for by their normal respiratory balance [10]. If all the wet-weight fluid was in the alveolar lumen, the mice would show respiratory distress. We hypothesize that some of this fluid may be accumulating in the interstitium.

HSC and NSC show differing responses to stimuli.

In addition to having different sensitivity to amiloride, NSC and HSC seem to respond differently to other environmental and pharmacological stimuli. Given the critical nature of the alveoli fluid layer, it would be evolutionarily beneficial to have two different types of channels that both contribute to the maintenance of AFC in response to different stressors. Relevant to the current study, Chen et al. observed that epithelial cells in cultures under hypoxic conditions decrease membrane density of HSC while increasing density of NSC [12]. Importantly, pulmonary edema can arise from changes in altitude that lead to low oxygen tension (HAPS-high altitude pulmonary syndrome). The decrease in partial pressure of oxygen leads to hypoxic pulmonary vasoconstriction and increased pulmonary vascular permeability. The

vasoconstriction results in higher hydrostatic pressure in the pulmonary capillaries that along with increased permeability drive excess fluid into the alveolar epithelium[13]. Impaired AFC may exacerbate this effect. Currently, we do not understand which of the two previously mentioned ion channels are implicated and lead to decreased AFC *in vivo*.

Additionally, the open probability of NSC increases in response to increased intracellular Calcium (Ca^{+}) in cell culture [7]. The open probability is a measure used in single-channel studies to indicate when ions can move across the channels and thus the contribution of that channel to AFC. Changes in intracellular calcium are induced by toxins from respiratory pathogens such as pneumolysin (PLY) in monolayers [14].

LPS and PLY have an impact on ENaC/HSC.

PLY is a toxin of Gram-positive bacteria that in cases of pneumonia is correlated with edema formation [15]. It is known to reduce the function of ENaC/HSC and to increase capillary endothelial permeability through its pore-forming activity [14]. Stringaris et al. found that this pore-forming activity allows an influx of Ca^{+} in neurons, but, to our knowledge, this mechanism has not, as yet, been described in alveolar epithelial cells [16]. We hypothesize that PLY's inhibitory action on ENaC/HSC is regulated through the calcium-induced phosphorylating action of Protein Kinase C (PKC). PKC is known to block ENaC/HSC's function which secondarily reduces alveolar fluid clearance.

Similarly, Lipopolysaccharide (LPS) is an endotoxin characteristic of Gram-negative bacteria. LPS induces an immune response, blocks ENaC/HSC in humans, and increases intracellular calcium [17]. Additionally, LPS stimulates the production of superoxide, a reactive oxygen species (ROS). ROS at high concentrations can damage ion channels, such as

ENaC/HSC, and ultimately affect fluid regulation [18]. Taken together, these observations suggest that one possible mechanism for the occurrence of alveolar flooding is mediated by ROS. The activation of PKC is also observed after bacteria-induced production of LPS in human monocytes, but the same mechanism has not been confirmed in human alveoli [19]. Despite ample research on the impact of LPS and PLY on ENaC/HSC, not much is known about their impact on NSC [20-23].

PLY impairs epithelial and endothelial function.

In addition to inhibiting the function of apical ENaC/HSC, Lucas et al. observed that intratracheal instillation of PLY resulted in hyperpermeability of lung microvascular endothelial cells and lung pulmonary artery endothelial cells [24]. PLY is found to cause impairment of pulmonary microvascular barrier function and severe pulmonary hypertension [15]. Taken together, research shows that the increase in alveolar fluid that is characteristic of pulmonary edemas may result from both disruption of the fluid return mechanism and an initial increase in the amount of fluid entering the lumen from the interstitium. Although these studies have proposed several mechanisms that result in hyperpermeability, including disruption of microtubule dynamics [24], we hypothesize that HSC and NSC are likely also involved.

ENaC/HSC is thought to contribute significantly to vascular function as it has been described in the endothelium and vascular smooth muscle [25-27]. Specifically, studies show that α-ENaC contributes to vascular endothelial function as endothelial cells in culture without α-ENaC show inflammation presumably mediated through changes in nitric oxide (NO) [14, 25]. Given these previous findings and the presence of α-ENaC in both NSC and HSC, it is possible

that the mechanism of vascular barrier impairment caused by PLY is through disruption of cation channels. It is important to elucidate this pathway *in vivo*.

Study aims.

In this study, we aim to test several hypotheses about the contribution of nonselective cation channels to lung fluid regulation, alveolar epithelial permeability, and pulmonary capillary permeability. Additionally, we investigate the response of NSC to toxins from respiratory pathogens.

Using an animal model genetically modified to knock out ASIC1 subunit expression and consequently NSC, we examine the contribution of NSC to alveolar fluid clearance and barrier permeability. Furthermore, we introduce toxins to ASIC1 KO and wild type mice to understand mechanisms through which respiratory pathogens cause pulmonary edema.

We hypothesize that AFC will be lower in the absence of ASIC1a (ASIC1 KO) especially when exposed to LPS and PLY compared to the wild type control. Additionally, we hypothesize that ASIC1 KO animals will have increased baseline alveolar epithelium and pulmonary capillary permeability and that previously observed high wet-to-dry ratios will be explained by increased fluid in the interstitial space.

Despite ample research on the impact of toxins on HSC, not much is known about their impact on NSC. My experiments would allow us to begin understanding how the relationship between toxins and NSC cause changes in AFC. Through these experiments, we will determine if the impact of pathogens on epithelial ion channels mediates alveolar flooding in humans after bacterial infection in hopes of guiding future treatment.

Materials and Methods.

Animals.

A colony of ASIC1 knockout (KO) mice on a C57Bl6/N background was established at Emory University. We used C57Bl6/N strain of mice obtained from Jackson Laboratories as controls. Mice were housed on a 12-hour:12-hour light-dark cycle and fed standard laboratory chow with water ad libitum.

Mice used for experiments were of either sex and between 8 and 55 weeks of age. Mice were euthanized by an overdose of isoflurane via methods that conform to the recommendations of the American Veterinary Medical Association Panel on Euthanasia for humane euthanasia of mice. All protocols were approved by Emory University's Institutional Animal Care and Use Committee.

Chemicals and reagents.

We purchased all chemicals and reagents used from Sigma-Aldrich (St. Louis, MO) unless otherwise specified. Formamide, Ultra Pure 99.5% min, and Bovine Serum Albumin (BSA) were from Thermo Fisher (Waltham, MA).

Intratracheal Instillations.

Mice were anesthetized with 2-3% isoflurane until a toe-pinch elicited no reaction. The surgical area was prepared as described by Helms et al., then we made an incision in the anterior throat region of the mouse [28]. Using a 30G needle, 5 µl of instillate per gram of body weight were introduced into the upper respiratory tract using a 1-ml syringe. Instillates contained either 50 ng/ml PLY or 1 mg/ml LPS in PBS. A successful instillation was confirmed once the mice

showed a quick succession of a few shallow breaths. Once the intratracheal instillation was complete, the surgical incision was closed using 4-0 nylon suture and topical 2% Xylocaine (APP; Lake Zurich, IL) was applied. The mice were allowed to recover for 4 hours in solitary housing with food and water available ad libitum while half of the cage was under a heat lamp. After the 4-hour incubation period, mice were euthanized and AFC and/or alveolar epithelial permeability measures were performed using the methods described here.

Intraperitoneal Injections.

Mice were briefly anesthetized with 2-3% isoflurane until they stopped moving. Using a 27G needle, we administered intraperitoneal injections of LPS or PLY at a 30-40º angle, and pulled on the syringe to verify proper placement with no involvement of intestinal organs. The amount injected was 10 µl per gram of body weight as previously described [29]. The concentrations of LPS and PLY were the same as those used for intratracheal instillations, 50 ng/ml PLY or 1 mg/ml LPS in PBS. This method of toxin administration was used when Evans blue (EB) tail vein injections were going to be performed.

Alveolar fluid clearance.

We measured AFC in mice by filling their lungs with 0.7 ml of 5% BSA containing either 0.2 mg/ml Evans Blue (EB), EB and 10 µM amiloride, or an equimolar concentration of 40 kDa Fluorescein isothiocyanate–dextran (FITC). The FITC lavage fluid had a concentration of 8.3 mg/ml. The mice were euthanized via isoflurane overdose which was reached with 5% isoflurane until respiration ceased and a toe-pinch elicited no reaction. The mouse was placed under a heating lamp for the duration of the procedure. An incision was made on the anterior

throat region of the mouse and a trimmed, sterile 20G needle was placed caudally into the lumen of the exposed trachea. Using a nylon suture, the 20G needle was secured onto the trachea. The 5% BSA and dye solution was slowly instilled into the lungs using a 1 ml syringe. A 150 µl sample of the fluid was removed immediately after the initial instillation. After 15 or 30 minutes, the rest of the fluid was removed and the dye concentration (EB or FITC) of the t= 0 and t= 15 or 30 samples were measured. Undiluted samples were plated at 50 µl in triplicate with EB and FITC-dextran standards. EB and FITC concentrations were calculated with the help of standard concentrations prepared in PBS. Absorbance was measured at 620 nm for EB and 520 nm for FITC-dextran using a spectrophotometer (Synergy 2; BioTek) to determine the changes in concentration of these dyes.

AFC was calculated based on changes in the concentration of the instillate fluid using the formula, AFC= $[(V_i - V_f)/V_i]$ x 100. In this formula, V_i is the initial volume of the instillate (0.7 ml) and V_f is the final alveolar fluid volume. Thus, $V_f = (V_i \times D_i)/D_f$, where D is the concentration of Evans blue/ FITC-dextran in the instilled solution and D_f is the final concentration of Evans blue/FITC-dextran in the alveolar fluid [10, 30, 31]. This procedure was the same for PLY/LPS treated and untreated control and KO mice.

Evans blue capillary permeability assay.

Vascular permeability was measured in ASIC1 KO and wild type control mice using lateral tail vein injections with 250 µl of a 10 mg/ml Evans Blue (EB) in PBS solution as previously described [32, 33]. Before injections were administered, the mice were warmed under a heating lamp for five minutes to vasodilate the vasculature. The injections were performed using a sterile 30G needle and a successful injection was confirmed by looking for a vibrant blue

color of the mouse's nose and footpads within 2-3 minutes. An hour after EB administration, the mice were euthanized with an overdose of isoflurane. An incision was made in the anterior throat region and a trimmed, sterile 20G needle was placed caudally into the lumen of the exposed trachea. Bronchoalveolar lavage (BAL) fluid was collected by slowly inserting 700 µl of cold PBS through the 20G needle and lavaging twice as previously described [33, 34]. The chest cavity was opened and whole blood samples of about 100-250 µl were harvested via cardiac puncture from the right ventricle using a sterile 21G needle. Blood samples were centrifuged (1,000 g at 4°C) for 15 minutes and the serum was removed from the top. The lung was harvested, and the blood was flushed from the pulmonary vasculature via the right ventricle with approximately 10ml of PBS or until the lung tissue turned significantly whiter. Serum and supernatant were kept on ice or -20°C until analysis. The lungs were then dissected and any extra pulmonary tissue was cut. The lungs were incubated in 250 µl of Ultra Pure formamide at 60°C for 48 hours to extract the tissue Evans blue.

EB concentrations were calculated with the help of standard concentrations prepared in PBS ranging from 2×10^{-4} to 2 mg/mL EB. Blood serum with a 1:10 dilution, undiluted BAL, and undiluted incubated lung formamide were plated at 50 µl in triplicate with the EB standards. The absorbance of the samples was analyzed at 620 nm using a spectrophotometer (Synergy 2; BioTek). Vascular permeability measures were determined from the concentration of EB in BAL/EB in serum and EB in tissue/EB in serum. In both of these measures, EB in the serum is used to normalize EB in the samples. This procedure was the same for wild type control mice and mice treated with LPS or PLY.

Wet weight-to-dry weight ratios.

The whole lungs from ASIC1 KO and wild type mice were perfused and extracted using the same procedures described above. Wet weight (wet wt.) was determined by weighing the lungs immediately after removal. To obtain the dry weight (dry wt.), lungs were desiccated overnight at 110°C. The wet-to-dry ratio represents the amount of fluid in the lung and it was calculated by dividing the wet wt. by the dry wt [10]. A larger ratio indicates larger fluid volumes in the lung.

Alveolar epithelial permeability.

We analyzed alveolar epithelial permeability in mice by filling their lungs with 0.7 ml of 5% BSA containing equimolar concentrations of 40, 20, and 10 kDa Fluorescein isothiocyanate–dextran (FITC-dextran). The different FITC-dextran fluids had concentrations of 8.3, 4.2, and 2.1 mg/ml. The mice were euthanized via isoflurane overdose which was reached with 5% isoflurane until respiration ceased and a toe-pinch elicited no reaction. The mouse was placed under a heating lamp. An incision was made on the anterior throat region of the mouse and a trimmed, sterile 24G needle was placed caudally into the lumen of the exposed trachea. Using a nylon suture, the 24G needle was secured onto the trachea. The 5% BSA and FITC-dextran solution was slowly instilled into the lungs using a 1 ml syringe. A 150 µl sample of the fluid was removed immediately after the initial instillation. After 30 minutes, the rest of the lavage fluid was removed and the FITC-dextran concentration of the t= 0 and t= 30 samples was measured. After the second sample (t= 30) was collected, whole blood samples of about 100-250 µl were harvested via cardiac puncture from the right ventricle using a sterile 21G needle. The blood was allowed to clot while in indirect contact with ice for 30 minutes. Then, blood samples were

centrifuged (1,000 g at 4°C) for 10 minutes and the serum was removed from the top. The lung was harvested, and blood was flushed from the pulmonary vasculature via the right ventricle with approximately 10 ml of cold PBS or until the lung tissue turned significantly whiter. The lungs were then dissected and any extra pulmonary tissue was cut away. The lungs were incubated in 250 µl of Ultra Pure formamide at 60°C for 48 hours.

FITC-dextran concentrations were calculated with the help of standard concentrations prepared in PBS. Undiluted lavage fluid, blood serum with a 1:5 dilution in PBS, and undiluted lung formamide were plated at 50 µl in triplicate with the corresponding FITC-dextran standards on a 96-well plate. The absorbance of the samples was analyzed at 520 nm using a spectrophotometer (Synergy 2; BioTek) to determine the FITC-dextran concentrations. This procedure was the same for PLY/LPS treated versus untreated control and KO mice. [35].

Single-channel, patch-clamp analysis.

We used patch-clamp electrophysiology to assess HSC and NSC activity in AT2 cells isolated from ASIC1 KO and C57B16/N control mice. Primary alveolar epithelial type II (AT2) cells were isolated from ASIC1a knockout and C57Bl6 control mice, as previously described [36, 37]. Cell-attached patch-clamp recordings of single-channel currents from AT2 cells were carried out using an Axopatch 1D amplifier at room temperature (22-25°C) (Molecular Devices, Sunnyvale, CA). AT2 cells were prepared on a permeable support prior to single-channel patch-clamp, as previously described for patch-clamp of cells in culture [12, 38].

Lung slices were also used. After euthanasia, lungs were filled with low meting point agar. Lungs were removed *en bloc* and perfused free of blood with ice cold PBS. A small piece of the lower left lobe was mounted on the table of a vibratome and 250 µm slices were placed

into 37^{o} C PBS. Slices were mounted in a chamber on the stage of the patch clamp microscope after washing away agar. Briefly, a microelectrode was filled with physiological buffer and applied to a single cell using suction, until a greater than 1 GΩ seal was formed. ENaC/HSC or NSC channels were identified by characteristic channel kinetics and the current-voltage relationship for the channel [10].

Single-channel currents were obtained with different applied pipette potentials, filtered at 1 kHz, and sampled every 50 μs with Clampex 10 software (Molecular Devices, Sunnyvale, CA, USA). All experiments were conducted at room temperature. The total number of functional channels in the patch was estimated by observing the number of peaks detected on the current amplitude histograms during at least a 10-minute recording period. To compare the difference in channel activity between control and treated groups, the open probability (P_O) of HSC and NSC channels was calculated using Clampfit 10. Channel density (N), Channel open probability (P_o), and Current/Voltage (I/V) relationship were calculated as previously reported [39].

Statistical analysis.

Statistical analysis was performed using SigmaPlot software. Statistical significance between groups was determined using paired or unpaired t-tests, as appropriate. One-way ANOVA was used for experiments where the comparison between more than two groups was needed. Mann-Whitney ANOVA was used when normality was in doubt. Data are reported as means ± standard deviation. Results were considered significant if $p < 0.05$.

Results

NSC contribute about equally to AFC.

To determine the contribution of NSC to lung fluid regulation, we compared alveolar fluid clearance of wild type and ASIC1 knockout mice under various conditions. A one-way ANOVA indicated a significant difference in means between amiloride treated and untreated ASIC1 and control groups ($p < 0.001$; Figure 2). The data show that ASIC1 KO mice had decreased AFC compared to the wild type control ($36.0 \pm 0.40\%$ vs. $18.9 \pm 0.40\%$, $p < 0.001$ by Holm-Sidak; Figure 2). Pharmacological blockade of HSC with amiloride also resulted in a significant decrease in AFC compared to the control group ($36.0 \pm 0.40\%$ vs. 17.5 ± 0 .77%, $p < 0.001$ by Holm-Sidak; Figure 2). Both of these comparisons showed a drop of about half in AFC. Consistently, ASIC1 KO mice treated with HSC blocking amiloride had little to no AFC in 30 minutes ($1.41 \pm 0.17\%$; Figure 2). Control mice treated with amiloride and ASIC1 KO mice had statistically similar AFC ($17.5 \pm 0.77\%$ vs. $18.9 \pm 0.4\%$, $p = 0.50$ by Holm-Sidak; Figure 2).

Interestingly, in 15-minute AFC measures using EB the difference in AFC of control females and control males was statistically different ($10.92 \pm 3.24\%$ vs. $16.84 \pm 5.17\%$, $p < 0.001$ by t-test; Figure 3). However, AFC of ASIC1 males was not significantly different than AFC for ASIC1 KO females ($6.28 \pm 2.99\%$ vs. 4.92 ± 2.22 %, $p = 0.003$ by t-test; Figure 3).

Since our previous study has also shown that blocking HSC decreases AFC by half [10], these data support that each of the cation channels found in alveolar cells contributes to alveolar fluid regulation.

LPS and PLY block HSC-associated AFC.

We determined the impact of LPS and PLY on cation channels by looking at alveolar fluid clearance of control mice and ASIC1 KO mice after installation with these toxins. A Kruskal-Wallis test showed a significant difference between the treatment groups ($P< 0.001$; Figure 4). The data show that LPS significantly decreased AFC from 40.93 ± 8.14% (wild type control) to 17.25 ± 4.05% (wild type with LPS) ($p < 0.001$ by Holm-Sidak; Figure 4). Wild type mice treated with LPS and ASIC1 KO mice had statistically similar AFC (17.25 ± 4.05%, 20.95 ± 3.62%, $p = 0.10$ by Holm-Sidak; Figure 4). ASIC1 KO mice treated with LPS had a significantly decreased mean AFC of 6.76 ± 3.23% compared to the mean AFC of untreated ASIC1 KO, 20.95 ± 3.62% ($p < 0.001$ by Holm-Sidak; Figure 4).

Similarly, the data demonstrate that PLY reduced AFC of wild type control mice from 31.30 ± 5.83% to 14.15 ± 5.02% ($p < 0.001$ by Holm-Sidak; Figure 5). Wild type mice treated with PLY and ASIC1 KO mice had statistically similar AFC (14.154 ± 5.02% vs. 11.40 ± 2.53%, $p = 0.14$ by Holm-Sidak; Figure 5). However, ASIC1 KO mice treated with PLY had significantly lower AFC than untreated ASIC1 KO mice (2.78 ± 0.96% vs. 11.40 ± 2.53%, $p < 0.001$ by Holm-Sidak; Figure 5). The reduction of AFC caused by the introduction of the toxins suggests they are acting to inhibit HSC-related fluid clearance activity.

Acute PLY in alveolar type II cells suppresses HSC activity.

Using AT2 cells from C57B16/N control mice, we performed single-channel patch-clamp analysis to investigate how NSC and HSC open probability changes after treatment with pneumolysin. The data show that shortly after administration of PLY, the open probability of HSC significantly decreased from 0.64 ± 0.25% to 0.11 ± 0.05% ($p = 0.01$ by paired t-test;

Figure 6). Importantly, there was a significant acute increase in the open probability of NSC within four minutes of PLY introduction compared to the pre-PLY open probability (0.33 ± 0.10% vs. 0.06, ± 0.05%, $p = 0.01$ by paired t-test; Figure 6). This evidence for the inverse response of HSC and NSC to PLY is novel and may be helpful in guiding treatment.

ASIC1 KO mice have more fluid in their lungs.

We investigated the accumulation of fluid in the lungs of wild type control and ASIC1 KO mice using wet weight-to-dry weight ratios. The data suggest that ASIC1 KO mice have more fluid accumulation in their lungs as they had higher wet/dry ratios compared to the control group (6.01 ± 0.91 vs. 3.68 ± 0.34, $p < 0.001$ by Student's t-test and Welch's test; Figure 7).

Capillary permeability may be impacted by LPS.

The permeability of pulmonary capillaries was investigated using Evans Blue tail vein injections. A Kruskal-Wallis One Way Analysis of Variance on Ranks revealed that the differences in BAL/serum EB median values for the LPS treated and untreated ASIC1 KO and control groups were statistically different ($p < 0.001$; Figure 8A). Because these data are ratios, we report findings as median values ± inter-quartile ranges. The data show that the wild type group treated with LPS has a higher median ratio of EB in their bronchoalveolar lavage fluid to serum compared to the untreated control group (0.00073 ± 0.00044 vs. 0.0090 ± 0.0053, $p < 0.001$ by Dunn's Method; Figure 8A). The ASIC1 KO group treated with LPS also had higher median ratios of BAL/serum compared to the untreated control group (0.0088 ± 0.019, $p < 0.001$ by Dunn's Method; Figure 8A).

A Kruskal-Wallis One Way Analysis of Variance on Ranks revealed that the differences in tissue/serum EB median values for the treatment groups are statistically different ($p < 0.001$; Figure 8B). Interestingly, the data showed a statistical difference in median tissue/serum EB ratios between the LPS treated wild type group and the ASIC1 KO group (0.021 ± 0.012 vs. 0.070 ± 0.027, $p < 0.001$ by Dunn's Method; Figure 8B). No other comparison of group medians yielded a statistical significance; however, our data is preliminary and we hypothesize that more experiments are needed to reveal differences.

Forty KDa FITC-dextran is a measure of AFC.

We investigated FITC-dextran a tool for studying alveolar fluid regulation by conduction AFC measures using 40 kDa FITC-dextran. The data show similar trends of AFC as those collected with EB (Figure 8). Wild type mice treated with LPS had significantly lower median AFC compared to untreated wild type mice (19.37 ± 6.65 vs. 25.83 ± 14.04, $p < 0.05$ by Tukey Test; Figure 9). Treatment with PLY yielded a similar reduction in median AFC as measured by EB (14.07 ± 4.65 vs. 25.83 ± 14.04, $p < 0.001$; Figure 9).

FITC-dextran is a measure of epithelial permeability.

To further investigate alveolar epithelial permeability, we conducted AFC measures using 20 and 10 kDa FITC-dextran. Notably, measures using 10 kDa showed non-significant higher measures of AFC for untreated and PLY groups than 20 kDa and 40 kDa (Figure 10). Moreover, 20 kDa readings for the untreated, PLY, and LPS groups also had larger measures of AFC than the corresponding 40 kDa groups which are not significant but interesting. More sample points are required to see if the trend is meaningful.

To assess changes in the permeability of the alveolar epithelium caused by exposure to toxins from respiratory pathogens, we determined the ratio of FITC-dextran in lung tissue to FITC-dextran in the initial instillate using 40, 20, and 10 kDa FITC-dextran. An ANOVA followed by Holm-Sidak post-test showed that the difference in means among the eight treatment groups is statistically significant ($p < 0.05$; Figure 11); however, there are not enough samples to make any one significant although the overall effect is significant.

Discussion

Human respiration is dependent on the integrity of the alveoli. Dysregulation of the alveolar fluid layer caused by various pathologies including acute lung injury (ALI), pneumonia, and COVID-19 can lead to alveolar flooding—a potentially lethal outcome. Treatment of alveolar flooding is dependent on the diagnosis of the underlying cause as it determines how the alveoli have been impacted [40]. Consequently, it is critical to detail the physiological mechanism of the alveoli and how common respiratory pathogens disrupt them. Here, we describe how NSC and HSC channels are implicated during alveolar flooding.

NSC are significant contributors to lung fluid balance.

In recent years, the presence of two cation channels with differing structures (NSC and HSC) has been demonstrated and widely accepted [7, 41-44]; however, the prominent role of only ENaC/HSC in other sodium-transporting epithelia led to the dismissal of NSC as significant contributors to alveolar fluid clearance [45]. This study provides support for the critical role of nonselective cation channels in maintaining the alveolar fluid layer through the nonselective movement of cations.

Under normal physiological conditions, the lack of NSC after knocking out ASIC1 led to a ~50% reduction in the ability to clear fluid from the alveolar lumen from 36.0 ± 0.39% to 17.5 ± 0.77% ($p < 0.05$) (Figure 2). When HSC channels were pharmacologically inhibited, AFC also decreased by about half which is consistent with previous observations [46]. When we pharmacologically inhibited HSC in NSC knocked out mice, AFC was 1.41 ± 0.17% (Figure 2). This supports our hypothesis and previously observed measure of AFC in ASIC1 KO mice [10].

Taken together, these results allow us to estimate that each cation channel contributes about equally to the return of fluid to the interstitial through the movement of different cations.

Our data showed a bimodal distribution of our AFC data, and upon further analysis observed a significant difference between wild type mean female and mean male AFC (10.92 ± 3.24% vs 16.84 ± 5.17%, $p < 0.001$; Figure 3). This observation suggests that there may be sex differences in ENaC/HSC function or expression. Although this is a very preliminary observation, it supports previous findings that male fetal distal lung epithelial cells show reduced sodium transport compared to female cells in culture [47]. Secondary to decreased sodium transport would be reduced AFC which we observed in our *in vivo* model. Further research is needed to understand this correlation.

LPS and PLY act on ENaC/HSC to inhibit fluid clearance.

Not only do NSC contribute to alveolar fluid clearance, the current study shows that their role is critical under stress caused by respiratory pathogens. Despite having significantly decreased alveolar fluid clearance, mice not expressing NSC look relatively healthy and show no signs of distress under normal housing conditions. However, as we hypothesized, introducing lipopolysaccharide or pneumolysin to the lungs of KO mice significantly reduces their ability to clear fluid and induce noticeable signs of respiratory distress.

Wild type mice instilled with LPS showed AFC statistically comparable to that of mice without NSC (17.25 ± 4.05%, 20.95 ± 3.62%, $p = 0.10$; Figure 4). The mean AFC of NSC knockout mice is 6.76 ± 3.23% which is significantly lower than the previously mentioned groups ($p < 0.001$). The drop in AFC suggests that LPS leads to alveolar flooding in mice by blocking HSC-related fluid clearance. Despite the significant drop in AFC, there is still a

movement of fluid out of the alveolar lumen. We speculate that this is a result of the LPS dose used not inhibiting all HSC channels. Thus, this study tells us that LPS's production of ROS may be selectively acting on HSC as NSC-related AFC persists in wild type mice instilled with LPS. Lung injury in mice induced by LPS is often used to model ALI in humans as the immunopathogenesis is similar; thus, our findings can help guide treatment for alveolar flooding arising from this cause [48]. Moreover, LPS is persistently found in the environment, so it is clinically relevant to understand how it impacts airway function [49].

As described, we hypothesize that pneumolysin has a similar impact of increasing ROS as LPS; therefore, it is not surprising that instilling wild type mice with PLY results in a mean AFC less than half of the mean AFC of untreated wild type mice (31.30 ± 5.83% vs.14.15 ± 5.02% ($p < 0.001$; Figure 5). As with LPS, when mice not expressing NSC are instilled with PLY, almost all AFC is eliminated (2.78 ± 0.96). PLY is released by pneumonia-causing bacteria and can induce pulmonary edema days after the start of antibiotic therapy [15, 50]. Given this drastic pathophysiological response, it is crucial to understand PLY's impact on alveolar fluid regulation. Lung injury induced by PLY is not thought to be a result of changes in phagocytic cells but rather its impact on the alveolar-capillary barrier [51]. In this study, we show that PLY is particularly inhibiting fluid clearance facilitated by HSC while sparing NSC-related fluid clearance.

NSC and HSC have contrasting responses to acute PLY.

NSC and HSC have been observed to have seemingly opposite reactions to various stimuli including purinergic stimulation and hypoxia [12, 52-54]. Single-channel clamp patch analysis in our study reveals a similar pattern but the effect is extremely acute. HSC open

probability decreased from 0.64 ± 0.25% to 0.11 ± 0.05% while NSC open probability increased from 0.33 ± 0.10% to 0.06, ± 0.05% ($p < 0.001$) (Figure 6). These probabilities were determined in a four-minute period after PLY introduction in cultured cells; however, four hours later when AFC measures are collected from mice, there is no evidence of NSC activity up-regulation as AFC is still only ~50% that of the control group (Figure 5). The decreased activity of HSC does persist.

Our findings contrast a previous study that observed an increase in open probability of HSC after acute application of LPS in AT1 cells [35]. This study hypothesized that the response was mediated by LPS –induced increases in ROS; however, we hypothesize this is also the downstream impact of PLY yet we observed the opposite response on open probability. In the future, we will repeat our experiments using LPS to gain more insight into this phenomenon. Although it is seemingly logical that the lungs' two cation channels would respond differently to physiological stimuli, we did not observe this to be true for extended periods following toxin-induced stress.

Endotoxins may compromise the integrity of epithelial barriers.

As discussed, efficient respiration is dependent on the homeostasis between the alveolar lumen, interstitial, and pulmonary capillaries. Normally there is no net change in the fluid entering and leaving the lumen as fluid exiting the capillaries is cleared to the lymphatic.

Consistent with previously observed wet weight-to-dry weight ratio of ASIC1 KO mice, we report larger ratios for ASIC1 KO mice compared to controls (6.01 ± 0.91 vs. 3.68 ± 0.34, $p < 0.001$; Figure 7) [10]. We theorized that fluid is accumulating in their interstitium since having

this much fluid in the lumen would manifest as respiratory distress, yet ASIC1 KO mice are seemingly healthy.

To further probe this observation and to confirm cell-culture findings of the contribution of HSC to pulmonary capillary integrity, EB was systemically circulated in mice and its concentration in the alveolar lumen and pulmonary tissue was observed. Differences in BAL/serum EB and tissue/serum EB concentrations between wild type and ASIC1 KO mice were not significant, but more experiments are being conducted. The current study does show that wild type and KO groups treated with LPS have more EB in their alveolar lumen compared to the untreated control group which we argue indicates an increase in capillary permeability (0.00073 ± 0.00044 and $.0088 \pm 0.019$ vs. 0.0090 ± 0.0053, $p < 0.001$; Figure 8A). In addition, LPS treated wild type mice have statistically lower EB in their pulmonary tissue than the untreated ASIC1 KO group which supports our hypothesis that fluid accumulates in the interstitial of ASIC1 KO mice as EB from the capillaries moves secondarily to fluid (0.021, 0.012 vs. 0.070, 0.027, $p < 0.001$; Figure 8B). Even with disruption of the capillary epithelium induced by LPS, untreated ASIC1 KO mice had higher capillary permeability which may suggest that NSC somehow contribute to the integrity and selectivity of the pulmonary capillary. Analysis of potential sex differences in these data are ongoing. As part of the alveolar system, this study also aimed to understand changes in alveolar epithelial permeability, especially after exposure to endotoxins.

Evans blue dye bound to albumin has a molecular weight of approximately 68 kDa and is known for its relatively poor movement across epithelial barriers. In contrast, studies on rat alveolar epithelial cells demonstrated that FITC-dextran with molecular weights up to 40 kDa can cross the alveolar epithelium through pores in paracellular pathways [55]. Thus, we

considered movement of these dye molecules as indicators of the alveolar epithelia's permeability to ions and small molecules that may influence the osmolarity of the different compartments.

Our permeability measures tracked FITC-dextran movement in the apical-to-basolateral direction using 40, 20, and 10 kDa FITC-dextran in treated (with LPS or PLY) and untreated wild type mice. We report that measures of AFC using 40 kDa FITC-dextran showed similar percentages of clearance as Evans Blue. Moreover, permeability measures of 40kDa FITC-dextran in pulmonary tissue showed a low accumulation of FITC-dextran (Figure 9; Figure 10). With these findings, we suggest that future measures of alveolar epithelial permeability should prioritize the use of smaller molecular weight Fluorescein isothiocyanate–dextrans.

Statistical analysis of the tissue to initial alveolar FITC-dextran concentration data revealed that the difference in means among the eight treatment groups is statistically significant ($p < 0.05$; Figure 11), but our sample sizes are too small to determine which groups differ significantly. Interestingly, we noticed a nonsignificant increase in AFC for PLY treated wild type mice as the size of the FITC-dextran decreased (Figure 9). It is possible that inflammation caused by PLY is driving FITC-dextran back into the alveolar lumen through the more permeable epithelial barrier created by PLY-induced ROS. More data points are needed to determine if this trend is actually representative of physiological mechanisms.

Summary: NSC are important for proper lung function, especially after endotoxin exposure.

Nonselective cation channels are key contributors to the maintenance of the alveolar fluid layer. Approximately half of the lungs' capacity to clear fluid is possible through the nonselective movement of cation channels via NSC.

Toxins from respiratory pathogens such as LPS and PLY disrupt the fluid layer predominantly through the inhibition of HSC. Simultaneously, NSC maintain the alveolar fluid layer thickness and thus respiration without a prolonged increase in their open probability. Conclusions about changes in alveolar epithelial permeability are limited by small sample sizes. The current study elucidates characteristics of the ASIC1 KO mouse model and investigates FITC-dextran as a tool for the study of mice epithelial integrity.

Our future aims include investigating the role of HSC in HAPE. Previous findings from our lab observed that NSC in culture are not as sensitive to oxygen reduction as HSC, so the next step will be to determine if this increased tolerance is present in the animal model by using ASIC1 knockout mice and wildtype mice

Current treatments for alveolar flooding are based only on mechanisms of alveolar fluid regulation by HSC with little consideration of the role of NSC channels. This study expands the paradigm on lung fluid regulation in hopes of guiding treatment for alveolar flooding caused by different pathologies and proposes future areas of inquiry to achieve this goal.

Figures

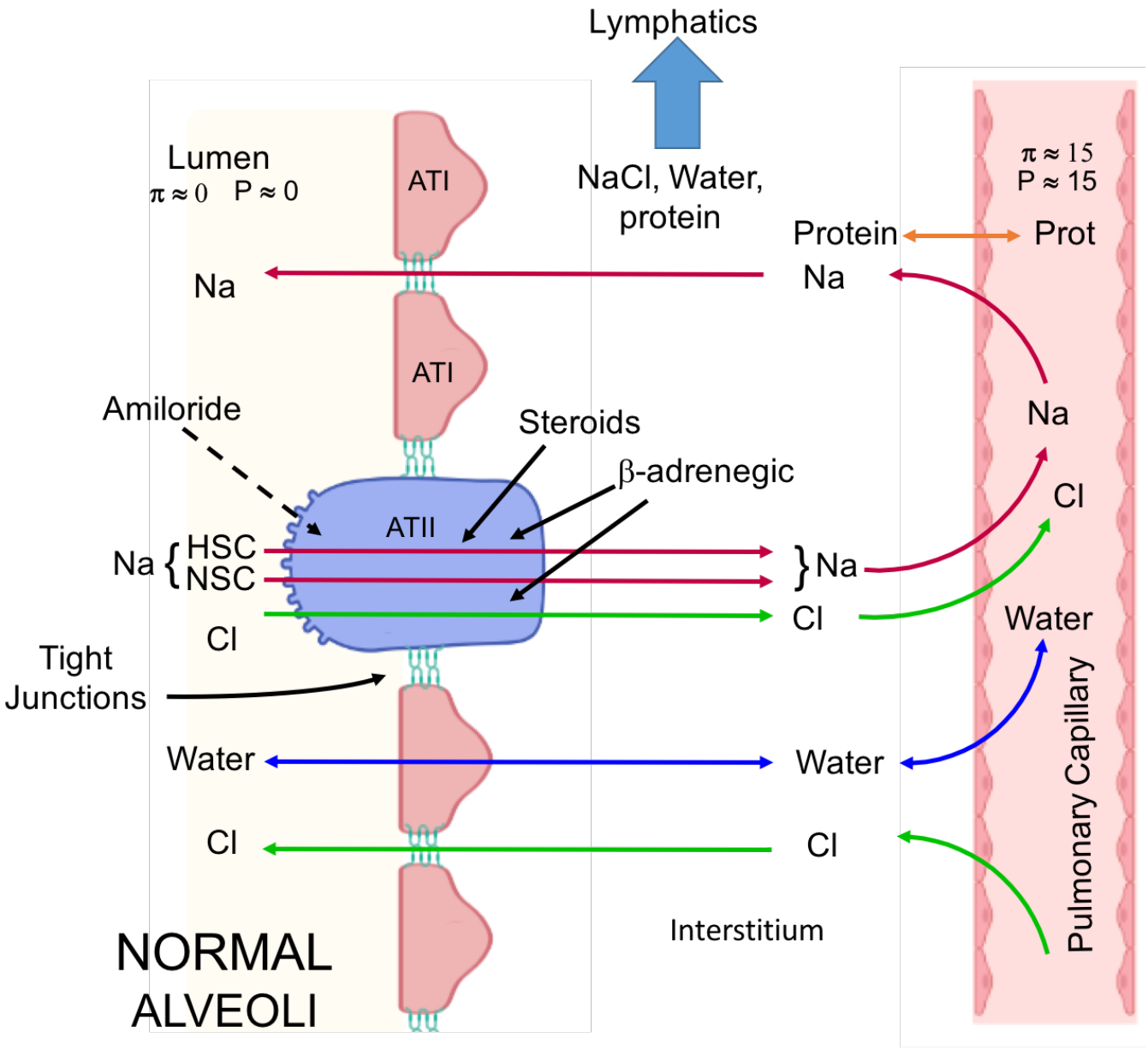

Figure 1. A schematic diagram of an alveolus. As depicted, human alveoli contain the alveolar lumen, the intercellular compartments of the polarized alveolar epithelial cells, tight junctions and the paracellular pathway, the basolateral interstitium, and the pulmonary capillaries' space. Salt and water move from the capillaries into the alveolus and then salt is actively transported back to the interstitium and capillaries to maintain fluid balance. Importantly, imbalance can lead

to alveolar dehydration or alveolar flooding. Both conditions can lead to potentially lethal compromise of blood oxygenation.

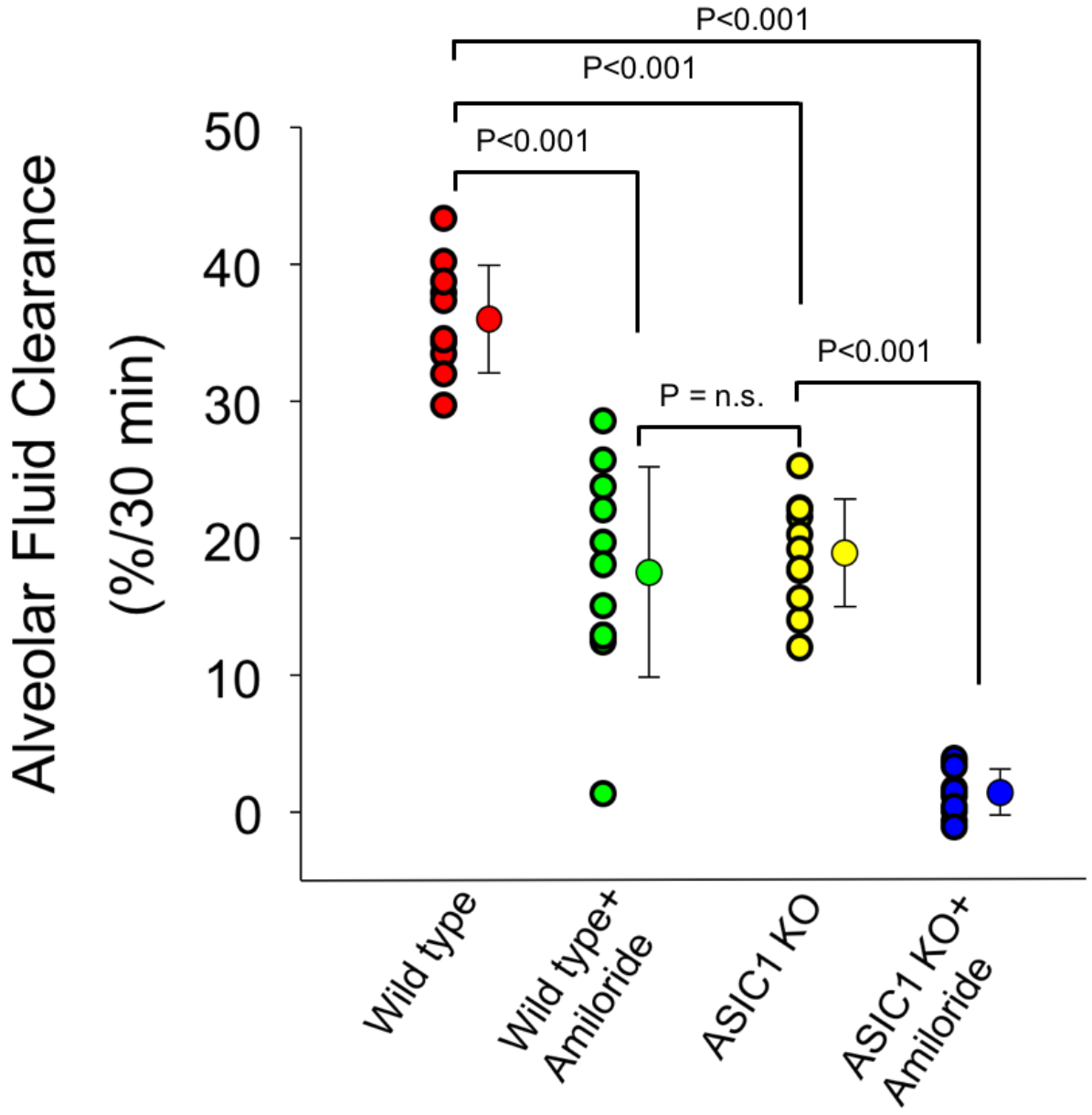

Figure 2. Genetic knockout of nonselective cation channels (NSC) and pharmacological blockage of highly-selective cation channels (HSC) decreases alveolar fluid clearance (AFC). ASIC1 KO mice have decreased AFC compared to the wild type (36.0 ± 0.40% vs. 18.9 ± 0.40%. AFC is significantly reduced after pharmacological blockade of HSC with amiloride compared to untreated wildtype (36.0 ± 0.40% vs. 17.5 ± 0 .77%). ASIC1 KO mice treated with HSC blocking amiloride have little to no AFC in 30 minutes (1.41 ± 0.17). Statistical comparison

is significant between all treatment groups at the $p < 0.001$ level except wildtype + amiloride versus ASIC 1 KO. The data represent $n = 11$ for each of the treatment groups; n.s., not significant.

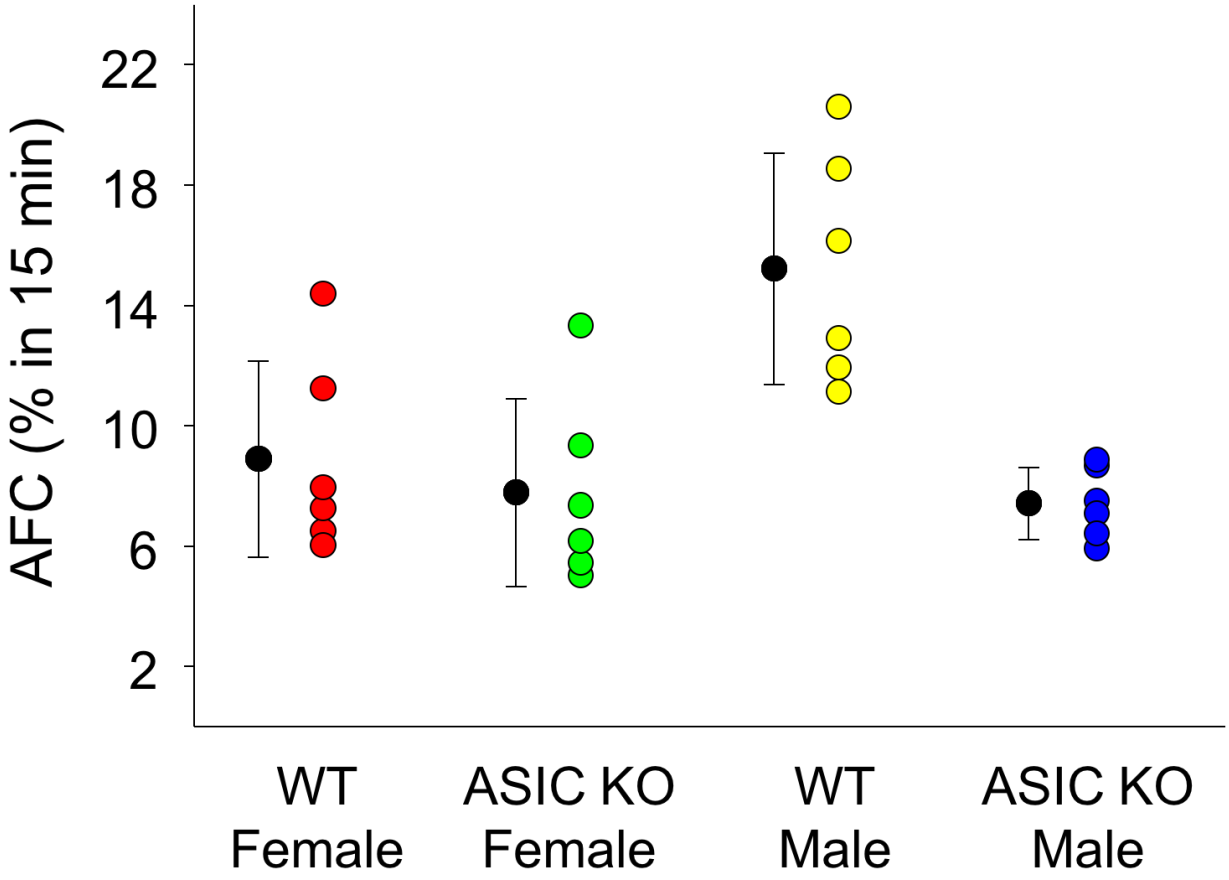

Figure 3. Highly-selective cation channel (HSC)-related fluid clearance is different in male and female wild type mice. Alveolar fluid clearance (AFC) of wild type (WT) males is significantly greater than AFC for WT females (n = 7 and n = 6, 16.84 ± 5.17% vs. 10.92 ± 3.24%. AFC of wild type (WT) males is significantly greater than AFC for ASIC1 KO males (n = 7 and n = 8, 16.84 ± 5.17% vs. 6.28 ± 2.999%, $p < 0.001$). Mean AFC for wild type females was significantly lower than mean AFC for ASIC1 KO females (n = 6 and n = 8, 10.92 ± 3.24 vs. 4.92 ± 2.22). Comparisons between all groups were statistically significant at the $p < 0.001$ level except the comparison between ASIC1 KO male and ASIC1 KO female AFC which was not significant.

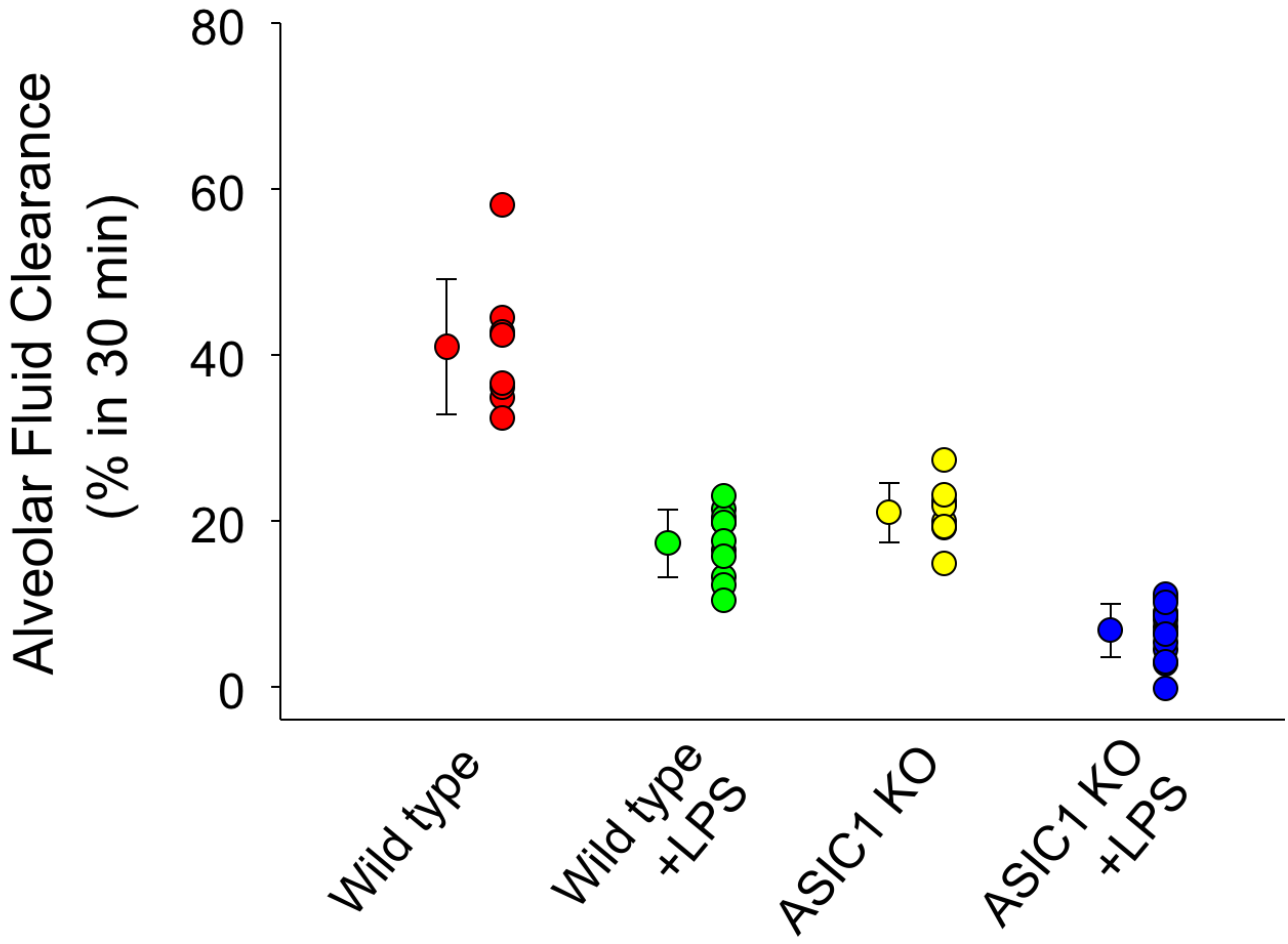

Figure 4. Lipopolysaccharide (LPS) inhibits highly-selective cation channel (HSC)-related alveolar fluid clearance (AFC). LPS in wild type mice significantly decreases AFC compared to the wild type group (n = 11, n = 8; 17.25 ± 4.05% vs. 40.93 ± 8.14%, $p < 0.001$). LPS in ASIC1 KO significantly decreased mean AFC compared to the untreated ASIC1 KO group (n = 15, n = 8; 6.76 ± 3.23% vs. 20.95 ± 3.62%, $p < 0.001$). Comparison between Wild type + LPS and ASIC1 KO groups yield no significant difference.

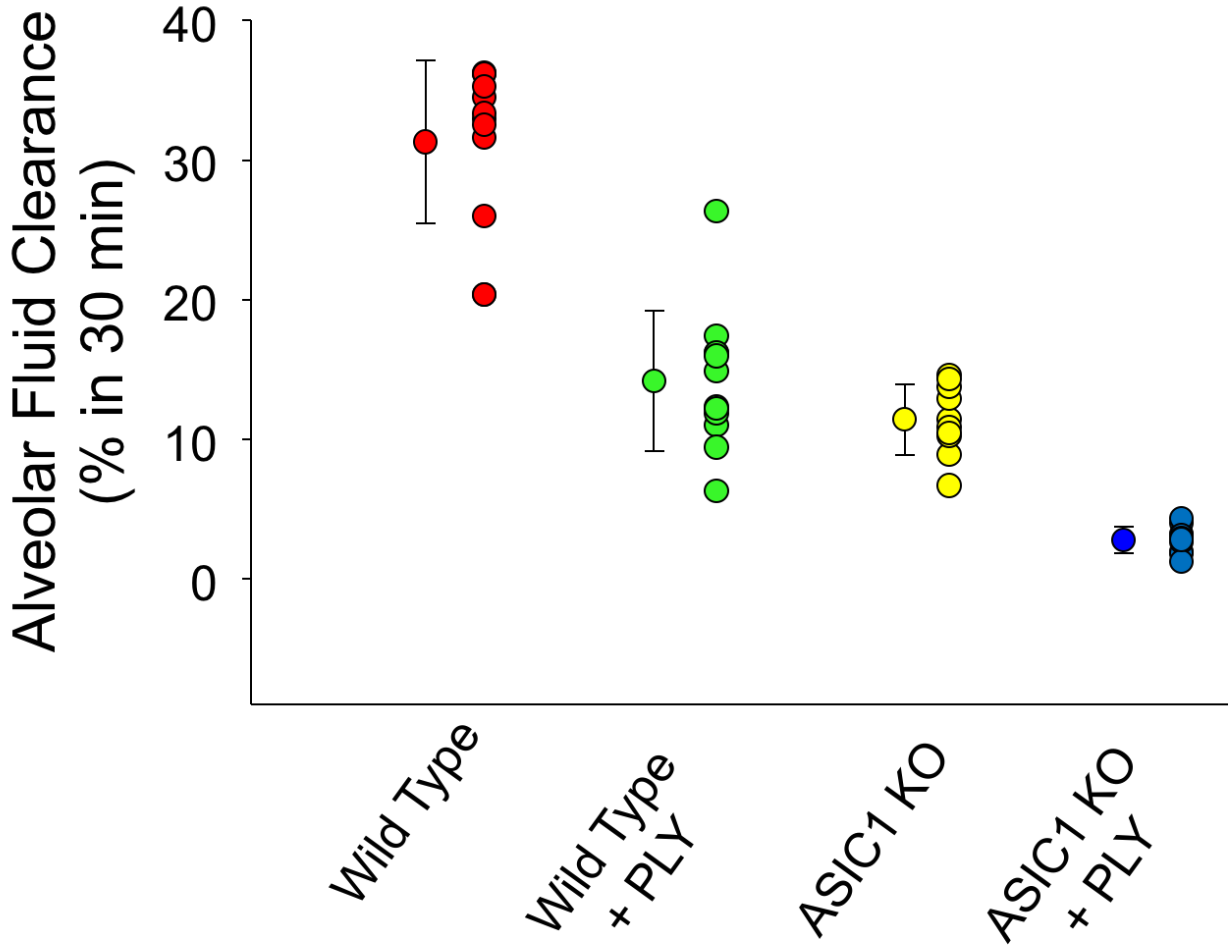

Figure 5. Pneumolysin (PLY) inhibits highly-selective cation channel (HSC)-related alveolar fluid clearance (AFC). AFC of wild type and PLY treated wild type are 31.30 ± 5.83% and 14.15 ± 5.02% respectively (n = 12 for each treatment group). AFC for the ASIC1 KO group decreases after treatment with PLY from 11.40 ± 2.53%, to 2.78 ± 0.96% (n = 10 for each treatment group. Comparison between all groups are significant at the $p < 0.001$ level except the comparison between Wild type + PLY and ASIC1 KO which is not significant.

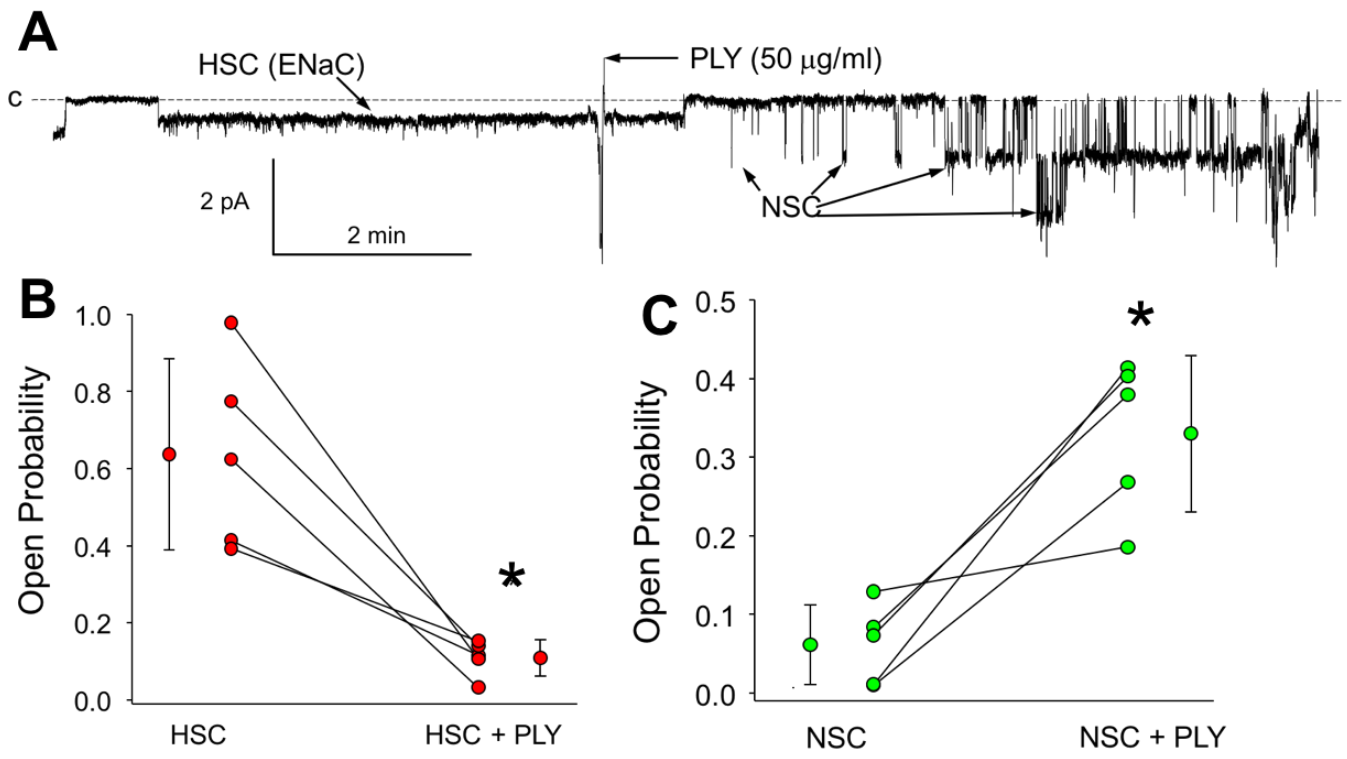

Figure 6. Pneumolysin (PLY) causes a significant increase in the open probability of nonselective cation channels (NSC) on alveolar type 2 cells as assessed by single-patch clamp analysis. (A) Distribution of current amplitudes in a patch on an AT2 cell. (B) The open probability of highly-selective cation channels (HSC) significantly decreases from 0.64 ± 0.25% to 0.11 ± 0.05% (n =5). (C) Open probability of NSC increases after PLY introduction compared to the pre-PLY open probability (0.33 ± 0.10% vs. 0.06, ± 0.05%, n = 5). Statistical analysis shows both comparisons are significantly different at the $p < 0.001$ level.

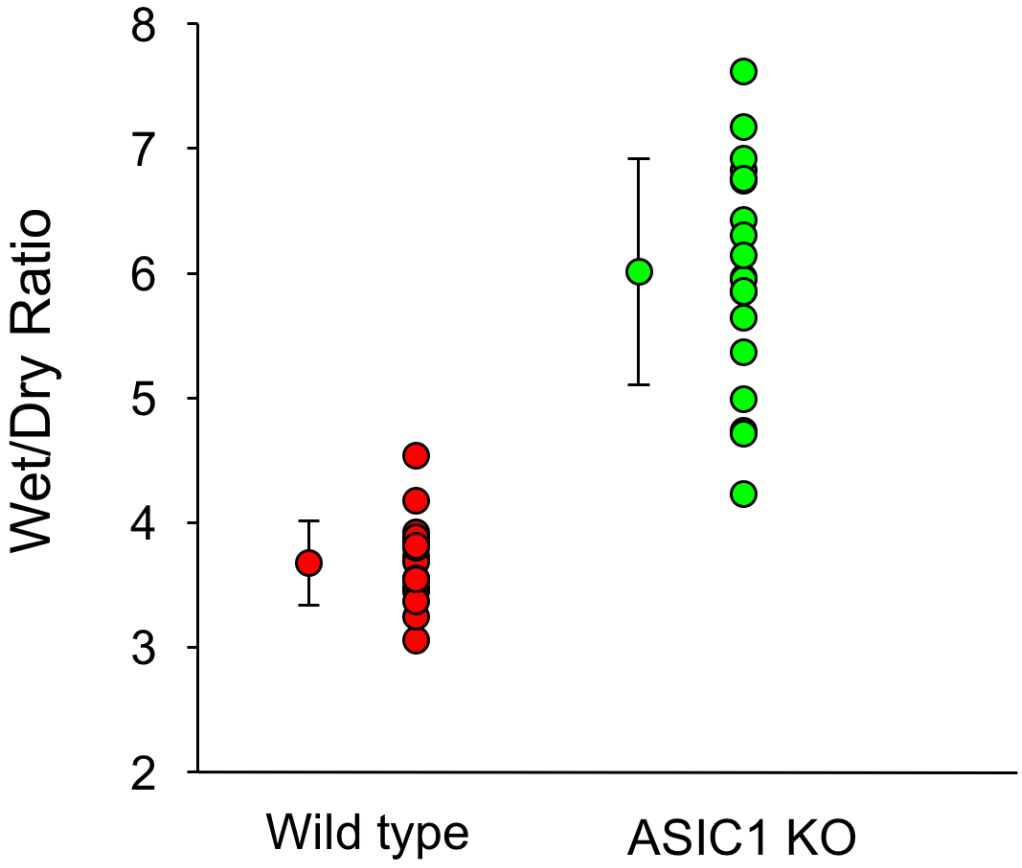

Figure 7. ASIC1 KO increases lung fluid content. ASIC1 KO mice have higher wet weight-to-dry weight ratios compared to the wild type group (n = 19 for each group, 6.01 ± 0.91 vs. 3.68 ± 0.34, $p < 0.001$)

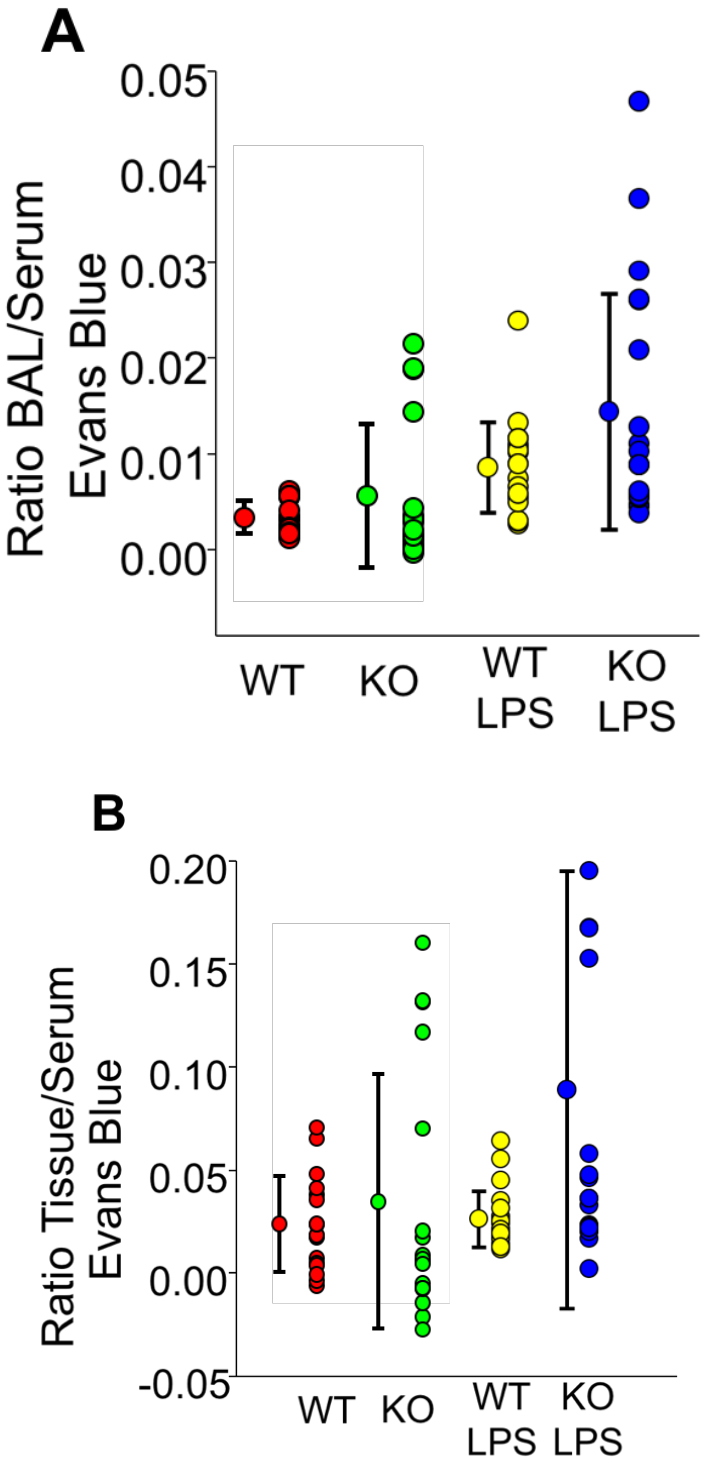

Figure 8. ASIC1 KO have fluid accumulation in their interstitium. Serum Evans blue was used to normalize the amount of EB that crossed the two barriers**.** (A) BAL/serum reveals EB

movement into the interstitial space. The wild type group treated with LPS has a higher median ratio of EB in their bronchoalveolar lavage fluid (BAL) to serum compared to the untreated wild type group (n = 21 and n = 9, 0.00073, 0.00044 vs. 0.0090, 0.0053). The ASIC1 KO group treated with LPS also had higher median ratios of BAL/serum compared to the untreated wild type group (n = 20, 0.0088, 0.019). Statistical analysis shows both comparisons are significantly different at the $p < 0.001$ level. (B) Median tissue/serum EB ratios between the LPS treated wild type group and the ASIC1 KO group are different (n = 21 and n = 8, 0.021, 0.012 vs. 0.070, 0.027). Statistical analysis shows that the comparisons described are significantly different at the $p < 0.001$ level. No other comparison of group medians yielded a statistical significance. Values are reported as median ± interquartile range

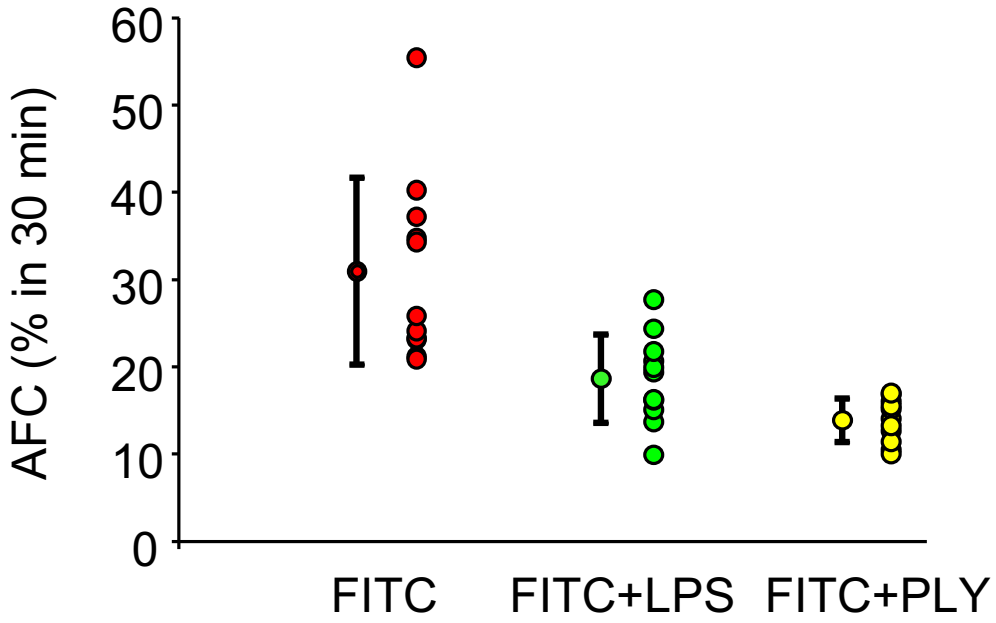

Figure 9. Forty KDa FITC-dextran detects decreases in fluid clearance caused by endotoxins alveolar fluid clearance (AFC) in wild type mice. Wild type mice treated with lipopolysaccharide (LPS) had significantly lower median AFC compared to untreated wild type mice (19.37± 6.65 vs. 25.83 ± 14.04, $p < 0.05$). Treatment with pneumolysin (PLY) yielded a similar reduction in median AFC as measured by EB (14.07 ± 4.65 vs. 25.83 ±14.04, $p < 0.001$).

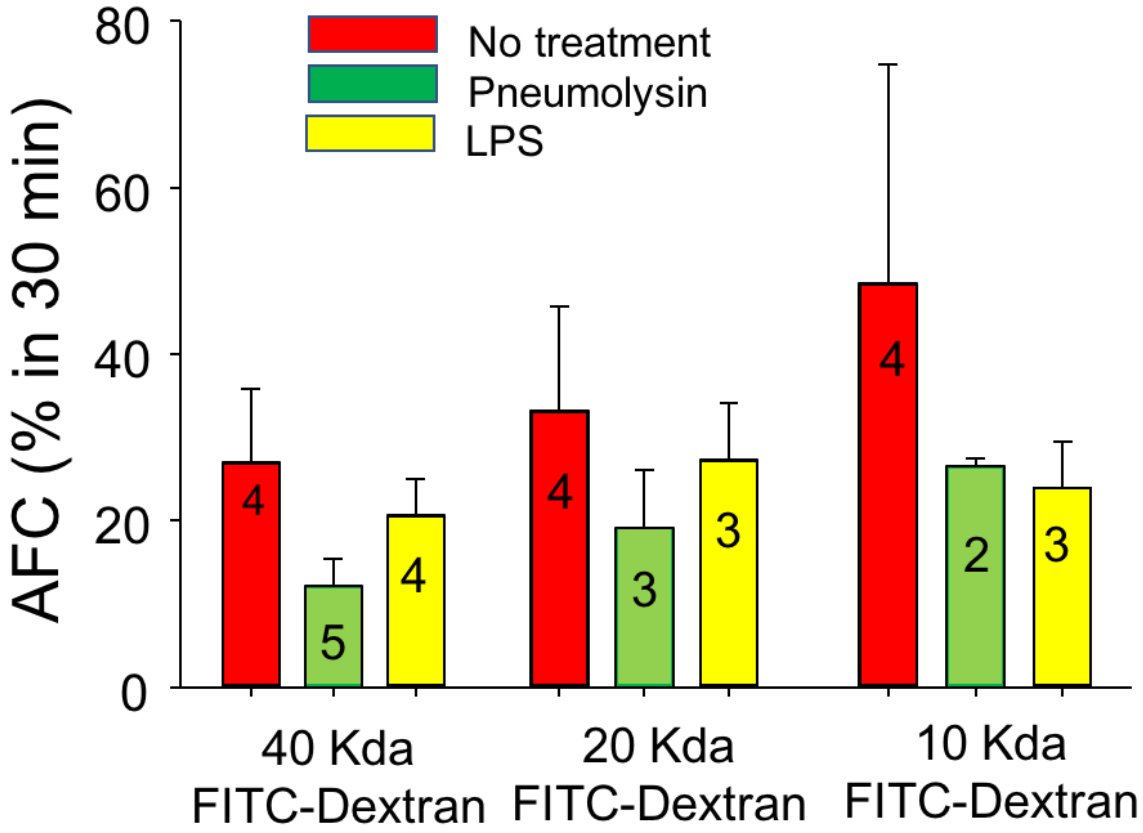

Figure 10. Different molecular weight FITC-dextran cross the alveolar epithelial to different degrees. The accumulation of dye using 20 kDa FITC-dextran on untreated, PLY, and LPS groups have larger measures of AFC than measures corresponding to the 40 kDa groups. The differences are not significant but interesting. No comparisons are significant. More data is needed.

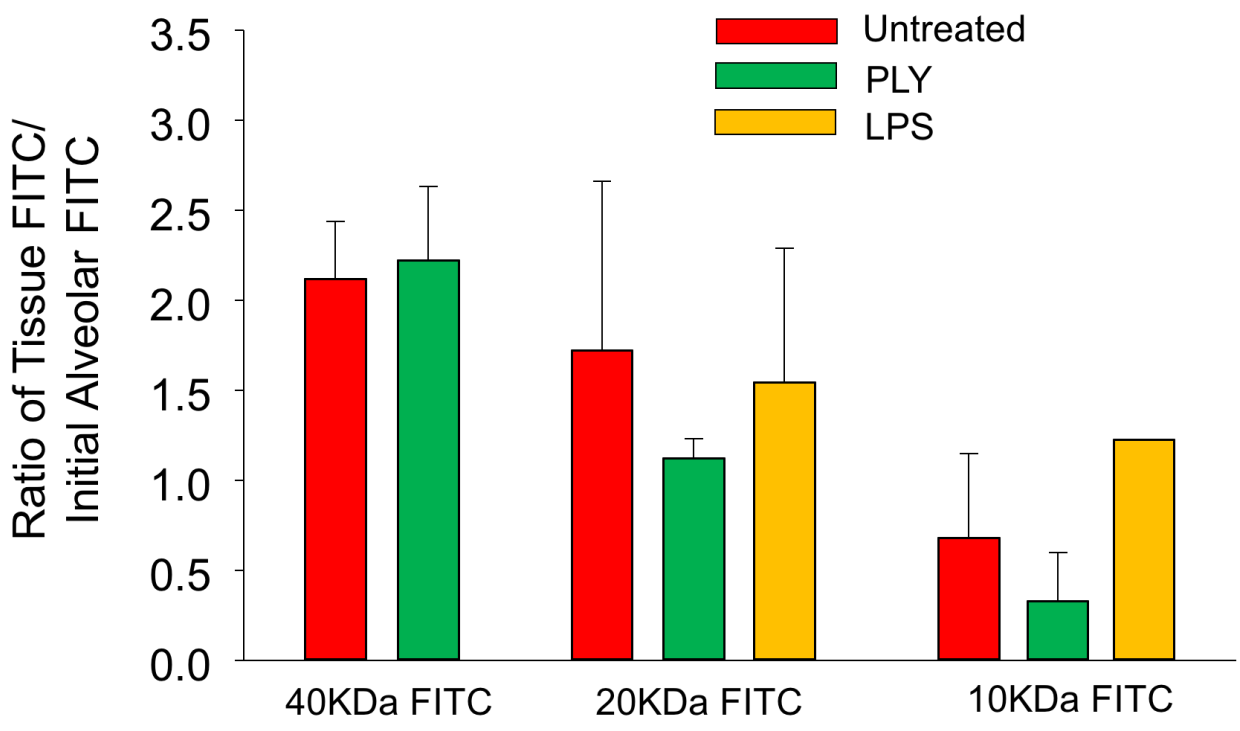

Figure 11. FITC-dextran is a measure of epithelial permeability. FITC-dextran in the tissue was normalized to the initial concentration in the alveolar lumen. A Holm-Sidak test shows that the difference in means among the eight treatment groups is statistically significant ($p < 0.05$); however, there are not enough samples to determine which groups are significant although the overall effect is significant.

References

1. Boucher, R.C., *Airway Surface Dehydration in Cystic Fibrosis: Pathogenesis and Therapy.* Annual Review of Medicine, 2007. **58**(1): p. 157-170.

2. Fronius, M., W. Clauss, and M. Althaus, *Why Do We have to Move Fluid to be Able to Breathe?* Frontiers in Physiology, 2012. **3**.

3. Tang, V.W. and D.A. Goodenough, *Paracellular ion channel at the tight junction.* Biophysical journal, 2003. **84**(3): p. 1660-1673.

4. Folkesson, H.G. and M.A. Matthay, *Alveolar epithelial ion and fluid transport: recent progress.* American journal of respiratory cell and molecular biology, 2006. **35**(1): p. 10-19.

5. Matthay, M.A., H.G. Folkesson, and C. Clerici, *Lung Epithelial Fluid Transport and the Resolution of Pulmonary Edema.* Physiological Reviews, 2002. **82**(3): p. 569-600.

6. Ware, L.B. and M.A. Matthay, *Alveolar Fluid Clearance Is Impaired in the Majority of Patients with Acute Lung Injury and the Acute Respiratory Distress Syndrome.* American Journal of Respiratory and Critical Care Medicine, 2001. **163**(6): p. 1376-1383.

7. Chen, X.-J., D.C. Eaton, and L. Jain, *β-Adrenergic regulation of amiloride-sensitive lung sodium channels.* American Journal of Physiology-Lung Cellular and Molecular Physiology, 2002. **282**(4): p. L609-L620.

8. Canessa, C.M., L. Schild, G. Buell, B. Thorens, I. Gautschi, J.D. Horisberger, and B.C. Rossier, *Amiloride-sensitive epithelial Na+ channel is made of three homologous subunits.* Nature, 1994. **367**(6462): p. 463-7.

9. Jain, L., X.-J. Chen, B. Malik, O. Al-Khalili, and D.C. Eaton, *Antisense oligonucleotides against the α-subunit of ENaC decrease lung epithelial cation-channel activity.* American Journal of Physiology-Lung Cellular and Molecular Physiology, 1999. **276**(6): p. L1046-L1051.

10. Trac, P.T., T.L. Thai, V. Linck, L. Zou, M. Greenlee, Q. Yue, O. Al-Khalili, A.A. Alli, A.F. Eaton, and D.C. Eaton, *Alveolar nonselective channels are ASIC1a/α-ENaC channels and contribute to AFC.* American Journal of Physiology-Lung Cellular and Molecular Physiology, 2017. **312**(6): p. L797-L811.

11. O'Brodovich, H., P. Yang, S. Gandhi, and G. Otulakowski, *Amiloride-insensitive Na+ and fluid absorption in the mammalian distal lung.* American Journal of Physiology-Lung Cellular and Molecular Physiology, 2008. **294**(3): p. L401-L408.

12. Jain, L., X.-J. Chen, S. Ramosevac, L.A. Brown, and D.C. Eaton, *Expression of highly selective sodium channels in alveolar type II cells is determined by culture conditions.* American Journal of Physiology-Lung Cellular and Molecular Physiology, 2001. **280**(4): p. L646-L658.

13. Stream, J.O., A.M. Luks, and C.K. Grissom, *Lung disease at high altitude.* Expert Review of Respiratory Medicine, 2009. **3**(6): p. 635-650.

14. Czikora, I., A.A. Alli, S. Sridhar, M.A. Matthay, H. Pillich, M. Hudel, B. Berisha, B. Gorshkov, M.J. Romero, J. Gonzales, G. Wu, Y. Huo, Y. Su, A.D. Verin, D. Fulton, T. Chakraborty, D.C. Eaton, and R. Lucas, *Epithelial Sodium Channel-α Mediates the Protective Effect of the TNF-Derived TIP Peptide in Pneumolysin-Induced Endothelial Barrier Dysfunction.* Frontiers in Immunology, 2017. **8**.

15. Witzenrath, M., B. Gutbier, A.C. Hocke, B. Schmeck, S. Hippenstiel, K. Berger, T.J. Mitchell, J.R. de los Toyos, S. Rosseau, N. Suttorp, and H. Schütte, *Role of pneumolysin for the development of acute lung injury in pneumococcal pneumonia.* Crit Care Med, 2006. **34**(7): p. 1947-54.

16. Stringaris, A.K., J. Geisenhainer, F. Bergmann, C. Balshüsemann, U. Lee, G. Zysk, T.J. Mitchell, B.U. Keller, U. Kuhnt, J. Gerber, A. Spreer, M. Bähr, U. Michel, and R. Nau, *Neurotoxicity of pneumolysin, a major pneumococcal virulence factor, involves calcium influx and depends on activation of p38 mitogen-activated protein kinase.* Neurobiol Dis, 2002. **11**(3): p. 355-68.

17. Kim, M., S.-W. Lee, J. Kim, Y. Shin, F. Chang, J.M. Kim, X. Cong, G.-Y. Yu, and K. Park, *LPS-induced epithelial barrier disruption via hyperactivation of CACC and ENaC.* Am J Physiol Cell Physiol, 2021. **320**(3): p. C448-c461.

18. Iles, K.E., W. Song, D.W. Miller, D.A. Dickinson, and S. Matalon, *Reactive species and pulmonary edema.* Expert Review of Respiratory Medicine, 2009. **3**(5): p. 487-496.

19. Shapira, L., S. Takashiba, C. Champagne, S. Amar, and T.E. Van Dyke, *Involvement of protein kinase C and protein tyrosine kinase in lipopolysaccharide-induced TNF-alpha and IL-1 beta production by human monocytes.* J Immunol, 1994. **153**(4): p. 1818-24.

20. Deng, W., C.-Y. Li, J. Tong, W. Zhang, and D.-X. Wang, *Regulation of ENaC-mediated alveolar fluid clearance by insulin via PI3K/Akt pathway in LPS-induced acute lung injury.* Respiratory Research, 2012. **13**(1): p. 29.

21. Ding, Y., Y. Cui, Z. Zhou, Y. Hou, X. Pang, and H. Nie, *Lipopolysaccharide Inhibits Alpha Epithelial Sodium Channel Expression via MiR-124-5p in Alveolar Type 2 Epithelial Cells.* BioMed Research International, 2020. **2020**: p. 8150780.

22. Dickie, A.J., B. Rafii, J. Piovesan, C. Davreux, J. Ding, A.K. Tanswell, O. Rotstein, and H. O'Brodovich, *Preventing Endotoxin-Stimulated Alveolar Macrophages from Decreasing Epithelium Na+ Channel (ENaC) mRNA Levels and Activity.* Pediatric Research, 2000. **48**(3): p. 304-310.

23. Lucas, R., S. Sridhar, F.G. Rick, B. Gorshkov, N.S. Umapathy, G. Yang, A. Oseghale, A.D. Verin, T. Chakraborty, M.A. Matthay, E.A. Zemskov, R. White, N.L. Block, and A.V. Schally, *Agonist of growth hormone-releasing hormone reduces pneumolysin-induced pulmonary permeability edema.* Proceedings of the National Academy of Sciences, 2012. **109**(6): p. 2084.

24. Lucas, R., et al., *Protein Kinase C-α and Arginase I Mediate Pneumolysin-Induced Pulmonary Endothelial Hyperpermeability.* American Journal of Respiratory Cell and Molecular Biology, 2012. **47**(4): p. 445-453.

25. Tarjus, A., M. Maase, P. Jeggle, E. Martinez-Martinez, C. Fassot, L. Loufrani, D. Henrion, P.B.L. Hansen, K. Kusche-Vihrog, and F. Jaisser, *The endothelial αENaC contributes to vascular endothelial function in vivo.* PLoS One, 2017. **12**(9): p. e0185319.

26. Tarjus, A., C. González-Rivas, I. Amador-Martínez, B. Bonnard, R. López-Marure, F. Jaisser, and J. Barrera-Chimal, *The Absence of Endothelial Sodium Channel α (αENaC) Reduces Renal Ischemia/Reperfusion Injury.* International journal of molecular sciences, 2019. **20**(13): p. 3132.

27. Kusche-Vihrog, K., P. Jeggle, and H. Oberleithner, *The role of ENaC in vascular endothelium.* Pflügers Archiv - European Journal of Physiology, 2014. **466**(5): p. 851-859.

28. Helms, M.N., E. Torres-Gonzalez, P. Goodson, and M. Rojas, *Direct Tracheal Instillation of Solutes into Mouse Lung.* JoVE, 2010(42): p. e1941.

29. Raduolovic, K., R. Mak'Anyengo, B. Kaya, A. Steinert, and J.H. Niess, *Injections of Lipopolysaccharide into Mice to Mimic Entrance of Microbial-derived Products After Intestinal Barrier Breach.* Journal of visualized experiments : JoVE, 2018(135): p. 57610.

30. Ware, L.B., X. Fang, Y. Wang, T. Sakuma, T.S. Hall, and M.A. Matthay, *Selected Contribution: Mechanisms that may stimulate the resolution of alveolar edema in the transplanted human lung.* Journal of Applied Physiology, 2002. **93**(5): p. 1869-1874.

31. Sakuma, T., M. Sagawa, M. Hida, Y. Nambu, K. Osanai, H. Toga, K. Takahashi, N. Ohya, and M.A. Matthay, *Time-dependent effect of pneumonectomy on alveolar*

epithelial fluid clearance in rat lungs. J Thorac Cardiovasc Surg, 2002. **124**(4): p. 668-74.

32. Radu, M. and J. Chernoff, *An in vivo assay to test blood vessel permeability.* Journal of visualized experiments : JoVE, 2013(73): p. e50062-e50062.

33. Smith, P., L.A. Jeffers, and M. Koval, *Measurement of Lung Vessel and Epithelial Permeability In Vivo with Evans Blue.* Permeability Barrier, 2021. **2367**: p. pp 137-148.

34. Van Hoecke, L., E.R. Job, X. Saelens, and K. Roose, *Bronchoalveolar Lavage of Murine Lungs to Analyze Inflammatory Cell Infiltration.* J Vis Exp, 2017(123).

35. Goodson, P., A. Kumar, L. Jain, K. Kundu, N. Murthy, M. Koval, and M.N. Helms, *Nadph oxidase regulates alveolar epithelial sodium channel activity and lung fluid balance in vivo via O2− signaling.* American Journal of Physiology-Lung Cellular and Molecular Physiology, 2012. **302**(4): p. L410-L419.

36. Dobbs, L.G., *Isolation and culture of alveolar type II cells.* Am J Physiol, 1990. **258**(4 Pt 1): p. L134-47.

37. Dobbs, L.G., R. Gonzalez, and M.C. Williams, *An improved method for isolating type II cells in high yield and purity.* Am Rev Respir Dis, 1986. **134**(1): p. 141-5.

38. Helms, M.N., X.-J. Chen, S. Ramosevac, D.C. Eaton, and L. Jain, *Dopamine regulation of amiloride-sensitive sodium channels in lung cells.* American Journal of Physiology-Lung Cellular and Molecular Physiology, 2006. **290**(4): p. L710-L722.

39. Marunaka, Y. and D.C. Eaton, *Effects of insulin and phosphatase on a Ca2(+)-dependent Cl- channel in a distal nephron cell line (A6).* J Gen Physiol, 1990. **95**(5): p. 773-89.

40. Matuschak, G.M. and A.J. Lechner, *Acute lung injury and the acute respiratory distress syndrome: pathophysiology and treatment.* Missouri medicine, 2010. **107**(4): p. 252-258.

41. Helms, M.N., J. Self, H.F. Bao, L.C. Job, L. Jain, and D.C. Eaton, *Dopamine activates amiloride-sensitive sodium channels in alveolar type I cells in lung slice preparations.* American Journal of Physiology-Lung Cellular and Molecular Physiology, 2006. **291**(4): p. L610-L618.

42. Lazrak, A., L. Chen, A. Jurkuvenaite, S.F. Doran, G. Liu, Q. Li, J.R. Lancaster, Jr., and S. Matalon, *Regulation of alveolar epithelial Na+ channels by ERK1/2 in chlorine-breathing mice.* Am J Respir Cell Mol Biol, 2012. **46**(3): p. 342-54.

43. Johnson, M.D., H.F. Bao, M.N. Helms, X.J. Chen, Z. Tigue, L. Jain, L.G. Dobbs, and D.C. Eaton, *Functional ion channels in pulmonary alveolar type I cells support a role for type I cells in lung ion transport.* Proc Natl Acad Sci U S A, 2006. **103**(13): p. 4964-9.

44. Lazrak, A., A. Samanta, and S. Matalon, *Biophysical properties and molecular characterization of amiloride-sensitive sodium channels in A549 cells.* American Journal of Physiology-Lung Cellular and Molecular Physiology, 2000. **278**(4): p. L848-L857.

45. Kirkman, E., *Fluid balance and non-respiratory functions of the lung.* Anaesthesia & Intensive Care Medicine, 2011. **12**(12): p. 527-529.

46. Flodby, P., Y.H. Kim, L.L. Beard, D. Gao, Y. Ji, H. Kage, J.M. Liebler, P. Minoo, K.-J. Kim, Z. Borok, and E.D. Crandall, *Knockout Mice Reveal a Major Role for Alveolar Epithelial Type I Cells in Alveolar Fluid Clearance.* American Journal of Respiratory Cell and Molecular Biology, 2016. **55**(3): p. 395-406.

47. Kaltofen, T., M. Haase, U.H. Thome, and M. Laube, *Male Sex is Associated with a Reduced Alveolar Epithelial Sodium Transport.* PLoS One, 2015. **10**(8): p. e0136178.

48. Rittirsch, D., M.A. Flierl, D.E. Day, B.A. Nadeau, S.R. McGuire, L.M. Hoesel, K. Ipaktchi, F.S. Zetoune, J.V. Sarma, L. Leng, M.S. Huber-Lang, T.A. Neff, R. Bucala, and P.A. Ward, *Acute lung injury induced by lipopolysaccharide is independent of complement activation.* Journal of immunology (Baltimore, Md. : 1950), 2008. **180**(11): p. 7664-7672.

49. Rylander, R., *Endotoxin in the environment--exposure and effects.* J Endotoxin Res, 2002. **8**(4): p. 241-52.

50. Rubins, J.B., D. Charboneau, C. Fasching, A.M. Berry, J.C. Paton, J.E. Alexander, P.W. Andrew, T.J. Mitchell, and E.N. Janoff, *Distinct roles for pneumolysin's cytotoxic and complement activities in the pathogenesis of pneumococcal pneumonia.* Am J Respir Crit Care Med, 1996. **153**(4 Pt 1): p. 1339-46.

51. Maus, U.A., M. Srivastava, J.C. Paton, M. Mack, M.B. Everhart, T.S. Blackwell, J.W. Christman, D. Schlöndorff, W. Seeger, and J. Lohmeyer, *Pneumolysin-induced lung injury is independent of leukocyte trafficking into the alveolar space.* J Immunol, 2004. **173**(2): p. 1307-12.

52. Davis, I.C. and S. Matalon, *Epithelial sodium channels in the adult lung--important modulators of pulmonary health and disease.* Adv Exp Med Biol, 2007. **618**: p. 127-40.

53. Ma, H.-P., L. Li, Z.-H. Zhou, D.C. Eaton, and D.G. Warnock, *ATP masks stretch activation of epithelial sodium channels in A6 distal nephron cells.* American Journal of Physiology-Renal Physiology, 2002. **282**(3): p. F501-F505.

54. Pochynyuk, O., V. Bugaj, A. Vandewalle, and J.D. Stockand, *Purinergic control of apical plasma membrane PI(4,5)P2 levels sets ENaC activity in principal cells.* American Journal of Physiology-Renal Physiology, 2008. **294**(1): p. F38-F46.

55. Matsukawa, Y., V.H.L. Lee, E.D. Crandall, and K.-J. Kim, *Size-Dependent Dextran Transport across Rat Alveolar Epithelial Cell Monolayers.* Journal of Pharmaceutical Sciences, 1997. **86**(3): p. 305-309.